

# A Point Mutation in Sec61 $\alpha$ 1 Leads to Diabetes and Hepatosteatorosis in Mice

David J. Lloyd,<sup>1,2</sup> Matthew C. Wheeler,<sup>3</sup> and Nicholas Gekakis<sup>3</sup>

**OBJECTIVE**—Type 2 diabetes is caused by both environmental and genetic factors. To better understand the genetic factors we used forward genetics to discover genes that have not previously been implicated in the development of hyperglycemia or diabetes.

**RESEARCH DESIGN AND METHODS**—Offspring of ethylnitrosurea-mutagenized C57BL/6 mice were bred to homozygosity, maintained on high-fat diet, and screened for hyperglycemia. The phenotype in one diabetic family of mice was mapped among hybrid F2s with single nucleotide polymorphic markers, followed by candidate gene sequencing to identify the gene harboring the causative mutation. Subsequent analysis was done on wild-type, heterozygous, and homozygous mutant mice on a pure C57BL/6 background.

**RESULTS**—Diabetes mapped to a point mutation in the *Sec61a1* gene that encodes a His to Tyr substitution at amino acid 344 (Y344H). Metabolic profiling, histological examination, and electron microscopy revealed that hyperglycemia was a result of insulin insufficiency due to  $\beta$ -cell apoptosis brought on by endoplasmic reticulum (ER) stress. Transgenic  $\beta$ -cell-specific expression of *Sec61a1* in mutant mice rescued diabetes,  $\beta$ -cell apoptosis, and ER stress. In vitro experiments showed that Sec61 $\alpha$ 1 plays a critical role in the  $\beta$ -cell response to glucose.

**CONCLUSIONS**—Here we phenotypically characterize diabetes in mice with a novel point mutation in a basic component of the cell's ER protein translocation machinery, Sec61 $\alpha$ 1. Translocation by the mutant protein does not appear to be affected. Rather, ER homeostasis is perturbed leading to  $\beta$ -cell death and diabetes. *Diabetes* 59:460–470, 2010

**T**ype 2 diabetes, a significant and growing cause of morbidity and mortality worldwide, is a result of defects in secretion of insulin and its effects on peripheral tissues. Epidemiological evidence makes it clear that  $\beta$ -cell deficiency, as measured by insulin secretion, is a risk factor for the development of type 2 diabetes (1). The precise nature of the  $\beta$ -cell defect that normally accompanies type 2 diabetes however remains unclear.

Although environmental factors have played a key role in the recent increases in type 2 diabetes, it is clear from

From the <sup>1</sup>Genomics Institute of the Novartis Research Foundation, San Diego, California; <sup>2</sup>Amgen, Thousand Oaks, California; and <sup>3</sup>The Scripps Research Institute, La Jolla, California.

Corresponding author: Nicholas Gekakis, gekakis@scripps.edu.

Received 3 October 2008 and accepted 30 October 2009. Published ahead of print at <http://diabetes.diabetesjournals.org> on 23 November 2009. DOI: 10.2337/db08-1362.

D.J.L. and M.C.W. contributed equally to this work.

© 2010 by the American Diabetes Association. Readers may use this article as long as the work is properly cited, the use is educational and not for profit, and the work is not altered. See <http://creativecommons.org/licenses/by-nc-nd/3.0/> for details.

The costs of publication of this article were defrayed in part by the payment of page charges. This article must therefore be hereby marked "advertisement" in accordance with 18 U.S.C. Section 1734 solely to indicate this fact.

epidemiological and recent genome-wide association studies that there is a strong genetic component (2–5). It is also apparent, from genome-wide association studies, that the genetic component of diabetes is spread across many genes, and that associations discovered to date are by no means an exhaustive list of genes that could carry polymorphisms that contribute to diabetes.

The strength of forward genetic screens lies in their ability to find novel genes involved in biological processes by focusing on specific phenotypes. Mutagenesis projects have been used in many model organisms such as yeast, *Drosophila*, worms, zebra fish, and, more recently, mice. Inducing germ-line point mutations by ethylnitrosurea (ENU) has led to the identification of genes involved in mammalian circadian rhythms (6), neuronal development (7), inflammation/autoimmunity (8), and cataract development (9). ENU mutagenesis has also been applied to the study of diabetes. Using ENU, Toyé et al. (10) isolated a mutation in glucokinase, a gene commonly mutated in maturity-onset diabetes of the young, indicating that this method has the potential to uncover genes that are physiologically relevant to the etiology of metabolic disorders.

In this report we describe a novel strain of diabetic mice, caused by an ENU-induced point mutation in *Sec61a1*. We found hyperglycemia to be temporally linked with  $\beta$ -cell loss and show a mechanistic link to endoplasmic reticulum (ER) stress-induced apoptosis. In addition to diabetes, these mice exhibit other metabolic abnormalities, including hyperlipidemia and hepatosteatorosis. In vitro experiments show that *Sec61a1* plays an important role in the  $\beta$ -cell response to ER stress and glucose. Although Sec61 is an essential gene in yeast, this study shows that a single amino acid alteration within one of the mammalian paralogs is not lethal and has profound metabolic consequences, most evident in the pancreatic  $\beta$ -cell.

## RESEARCH DESIGN AND METHODS

**Generation, housing, and diet of mice.** ENU-mutagenized C57BL/6J mice were generated as described (11). Mice were maintained by backcrossing affected animals to C57BL/6J and housed in the Genomics Institute of the Novartis Research Foundation Specific Pathogen-Free animal facility. All procedures were approved by the Genomics Institute of the Novartis Research Foundation Institutional Animal Care and Use Committee. Diets used in this study were chow (PicoLab Rodent Diet 20 no. 5053; LabDiet) and high-fat diet (HFD; D12331; Research Diets). Transgenic RIP-Sec mice were generated at the Scripps Research Institute by microinjecting linearized plasmid DNA into C57BL/6J pronuclei according to standard procedures.

**Phenotyping of mice.** Plasma from 4–6 h fasted mice was used for glucose, triglyceride, and cholesterol determination on a clinical blood chemistry analyzer (AU400e; Olympus). A duplicate sample was used for insulin enzyme-linked immunosorbent assay (Crystalchem). Nonfasted blood glucose was monitored using a OneTouch Ultra glucometer (LifeScan). Body composition analysis was performed using the EchoMRI-100 whole-body composition analyzer (EchoMRI).

**Mapping and genotyping.** Single nucleotide polymorphism assays ( $n = 356$ ) were performed using the Sequenom MassARRAY system as previously described (12). All exons of *Sec61a1* were amplified by PCR and sequenced for mutation detection. Specifically for genotyping, exon 10 was amplified

using the primers 5'-CGAATGACACCACAAGCATC-3' and 5'-CCAACTGTA GAATGGACGGC-3' and sequenced.

**Histology and immunohistochemistry.** Liver and pancreas were fixed in 10% phosphate-buffered formalin for 24 h and embedded in paraffin, and 5- $\mu$ m sections were prepared and stained using hematoxylin-eosin or Masson-Trichrome. Pancreatic sections were immunostained as previously described (13). Antibody combinations were as follows: rabbit anti-insulin (sc-9168; Santa Cruz Biotechnology) and AlexaFluor 594-conjugated chicken anti-rabbit antibody; goat anti-glucagon antibody (sc-97780; Santa Cruz Biotechnology) and AlexaFluor 488-conjugated donkey anti-goat antibody; goat anti-SEC61A1 antibody (ab1327; Abcam) and AlexaFluor 488-conjugated donkey anti-goat antibody; anti-immunoglobulin heavy chain-binding protein (BIP) antibody (sc-1050; Santa Cruz Biotechnology) and AlexaFluor 488-conjugated donkey anti-goat antibody; anti-C/EBP homologous protein (CHOP) antibody (sc-7351; Santa Cruz Biotechnology) and AlexaFluor 488-conjugated goat anti-mouse antibody. Fluorescent transferase-mediated dUTP nick-end labeling (TUNEL) staining was performed using the DeadEnd Fluorometric TUNEL System kit (G3250; Promega). All sections were stained with DAPI and mounted in Vectashield (Vector Labs).

**Pancreatic islet purification.** Pancreatic islets were isolated as previously described (13).

**Electron microscopy.** Isolated islets or dissected liver was processed for electron microscopy using a modification of the protocol by Gilula et al. (13a). Tissue was fixed in 4% paraformaldehyde, 1.5% glutaraldehyde in 0.1 M sodium cacodylate buffer (pH 7.3), washed and fixed in 1% osmium tetroxide/0.1 mol/l sodium cacodylate, subsequently treated with 0.5% tannic acid, followed by 1% sodium sulfate, buffer washed, and then dehydrated in graded ethanol. During the dehydration, islets were transferred to a microfuge tube for subsequent treatment. After incubation in propylene oxide and overnight infiltration in Epon/araldite, the resin pellets were polymerized at 60°C. Pellets were removed and reembedded in flat embedding molds. Thin sections (70 nm) were cut on a Reichert Ultracut E (Leica) using a diamond knife (Diatome; Electron Microscopy Sciences), mounted on parlodion-coated, copper slot grids, and stained in uranyl acetate and lead citrate. Sections were examined on a Philips CM-100 TEM (FEI, Hillsboro, OR) and data documented on Kodak SO-163 film.

**MIN6 cells, transfection, and thapsigargin.** MIN6 cells were obtained from Dr. J. Miyazaki, Osaka University, and cultured as described (14). Min6 cells were transfected with Lipofectamine 2000 according to package protocol (Invitrogen). ER stress-inducer thapsigargin was obtained from Sigma.

**Antibodies.** Mouse monoclonal anti-FLAG clone M2 and anti-insulin clone K36AC10 were purchased from Sigma. Rabbit polyclonal anti-pEIF2 $\alpha$  and mouse monoclonal total EIF2 $\alpha$  were obtained from Invitrogen. Western blot images were quantified using ImageJ software (National Institutes of Health).

**Metabolic labeling of insulin in Min6 cells and immunoprecipitation.** Min6 cells were maintained in high-glucose Dulbecco's modified Eagle's medium (DMEM) and transfected with the indicated construct in 35-mm dishes. Prior to labeling cells were starved for 30 min in Met- and Cys-free media and then pulsed with 50  $\mu$ Ci of easy tag express labeling mix for 30 min (Perkin Elmer). Cells were then chased for the indicated times in DMEM with 10% FBS. Cells were lysed in radioimmunoprecipitation assay buffer and immunoprecipitated with mouse monoclonal anti-insulin followed by the addition of Protein A/G (Calbiochem) agarose.

**Luciferase assay.** Min6 cells were transfected in triplicate in opaque, white 96-well plates. After 24 h, cells were treated with thapsigargin for 16 h. *Firefly* and *Renilla* luciferase activity was then determined using the Dual-Glo kit (Promega) and an Acquest luminometer (Molecular Devices).

**Quantitative RT-PCR.** All RNA was collected and extracted using an RNeasy kit (Qiagen). Quantitative PCR (qPCR) reactions were performed using SuperScript III Platinum One-Step qRT-PCR Kit (Invitrogen) and ABI PRISM 7900HT Sequence Detection System (Applied Biosystems, Foster City, CA) according to manufacturer's protocol. The reagents for analysis of mouse *Bip* were obtained as a commercially available Taqman Gene Expression Assay (Mm00517691\_m1). In MIN6 cells, *Sec61a1* was analyzed using the oligonucleotides 5'-TCAGCATCAGGGCCAGAT-3' and 5'-AGACAAGGCCACGTGT GATAT-3' and the probe 5'-CACACAGCCAGGGCGCACA-3'. In transgenic mice, *Sec61a1* was analyzed using a Taqman gene expression assay (Mm00489804\_m1) from Applied Biosystems. Expression values were normalized to a housekeeping gene *36B4*, which was analyzed using the oligonucleotides 5'-AGATGCAGCAGATCCGCAT-3' and 5'-GTTCTTGCCCATCAG CACC-3' and the probe 5'-CGCTCCGAGGGAAGGCCG-3'. Primers and probes for qPCR analysis of *Bip* and *Chop* in islets and livers were obtained from Applied Biosystems.

## RESULTS

**Identification of *Sec61a1* mutation and metabolic abnormalities in ENU-mutagenized mice.** In a forward-genetic screen using C57BL/6J mice, we identified a family of animals that exhibited hyperglycemia when fed a HFD. Affected mice were bred to 129/SvJ mice to generate hybrid F2s. A genome scan using single nucleotide polymorphisms in nine unaffected and four affected mice identified a 50-Mb locus on chromosome 6 (supplementary Fig. 1A, available in an online appendix at <http://diabetes.diabetesjournals.org/cgi/content/full/db08-1362/DC1>) that was inherited with the diabetic phenotype. Haplotype analysis of a further 140 F2 hybrid mice refined this locus to 4.7 Mb, between 88.1 and 92.8 Mb, a region containing 60 genes. We chose to sequence those genes enriched in pancreatic islets (<http://symatlas.gnf.org>), including *Sec61a1*. A homozygous missense mutation was identified within exon 10 of *Sec61a1* in affected animals (supplementary Fig. 1B). The T to C transition at codon 344 results in a Tyr to His (Y344H) amino acid substitution within Sec61 $\alpha$ 1.

Sec61 $\alpha$ 1 is highly conserved with orthologs from other animals and with the mouse paralog Sec61 $\alpha$ 2 (Fig. 1A). The Y344H mutation identified in the diabetic mice is localized to a double Tyr motif, present in all species analyzed, suggesting a crucial role for these two amino acids in Sec61 $\alpha$ 1 function. *Sec61a1*<sup>Y344H/Y344H</sup> mice exhibited hyperglycemia, most likely due to insulin insufficiency, as shown by hypoinsulinemia in the same mice (Fig. 1B, supplementary Table 1). Although heterozygous *Sec61a1* mice were not diabetic, they did display an intermediate hypoinsulinemic phenotype on HFD (Fig. 1B, supplementary Table 1). A time course of fasting blood glucose levels indicated that hyperglycemia appeared at an early time point in both males and females (Fig. 1C). This observation taken together with the profound hypoinsulinemia in mutant animals indicated that diabetes was due to  $\beta$ -cell failure.

Immunohistochemistry in pancreatic sections from normal mice confirmed islet expression of Sec61 $\alpha$ 1. Double staining of islets for Sec61 $\alpha$ 1 and insulin showed that Sec61 $\alpha$ 1 is highly expressed in  $\beta$ -cells (Fig. 1D). Surprisingly *Sec61a1* expression appeared much higher in islets than the surrounding acinar cells of the pancreas. qPCR, however, verified that islets exhibited an ~4.0-fold higher expression of *Sec61a1* compared with whole pancreas (Fig. 1E). A tissue survey of *Sec61a1* expression by qPCR revealed that *Sec61a1* was nevertheless expressed in whole pancreas at levels equal with many other tissues, affirming that Sec61 $\alpha$ 1 is expressed at exceptionally high levels in  $\beta$ -cells. Furthermore, qPCR performed on different tissues revealed that the  $\alpha$ 2 paralog was not expressed at higher levels in mutant mice than in wild-type mice and that the  $\alpha$ 2 paralog was expressed at relatively low levels in every tissue analyzed with the exception of whole brain (Fig. 1F).

Although diabetes was the most prominent phenotype in *Sec61a1*<sup>Y344H/Y344H</sup> mice, it was accompanied by multiple endocrinological and growth abnormalities (for both sexes on both chow and HFD; supplementary Table 1). *Sec61a1*<sup>Y344H/Y344H</sup> mice were smaller than wild-type littermates; both fat and muscle mass were reduced, 66 and 25%, respectively, in males fed a HFD (supplementary Table 1), resulting in 28% lower body weights. Also, *Sec61a1*<sup>Y344H/Y344H</sup> mice were hypercholesterolemic and

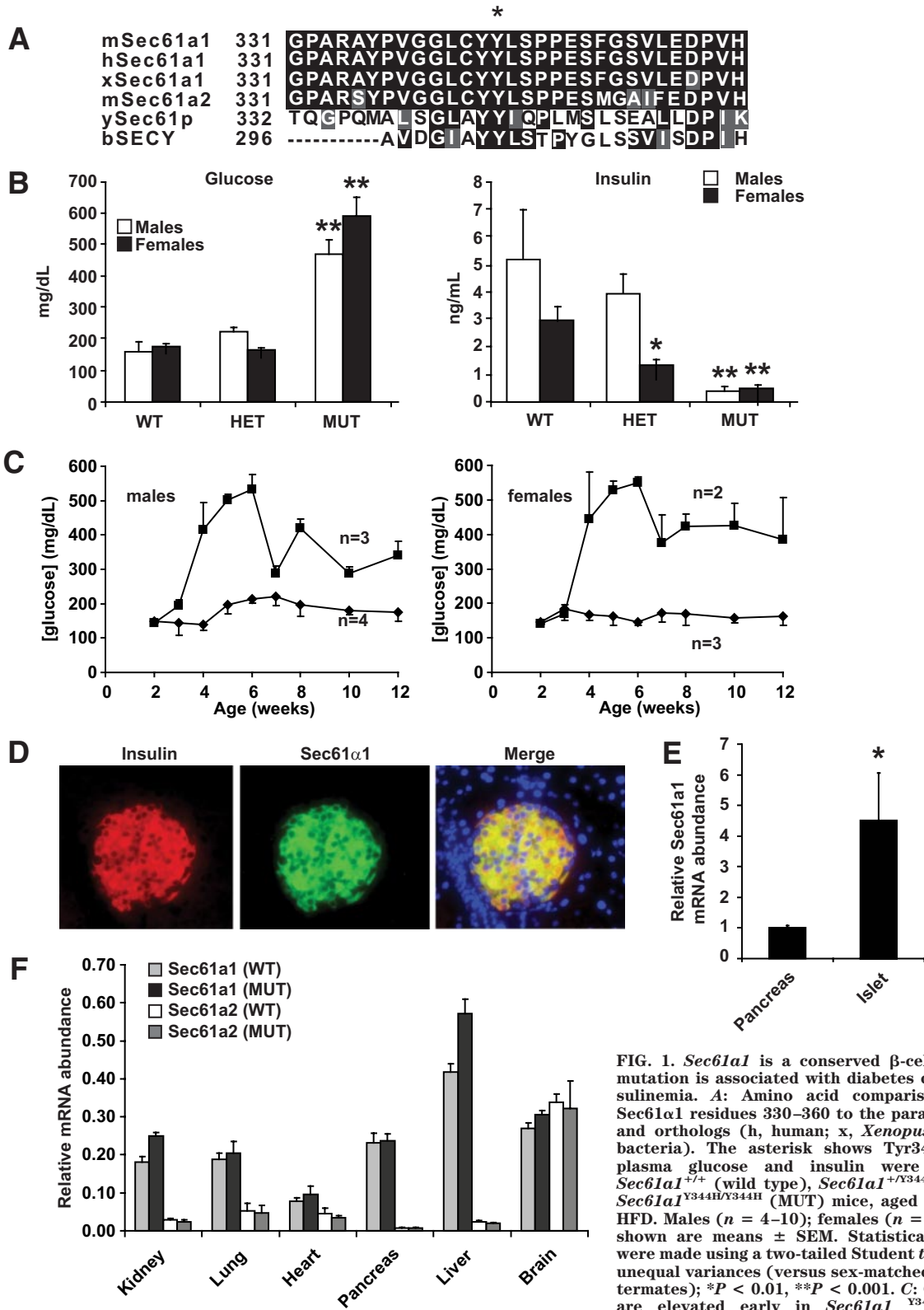
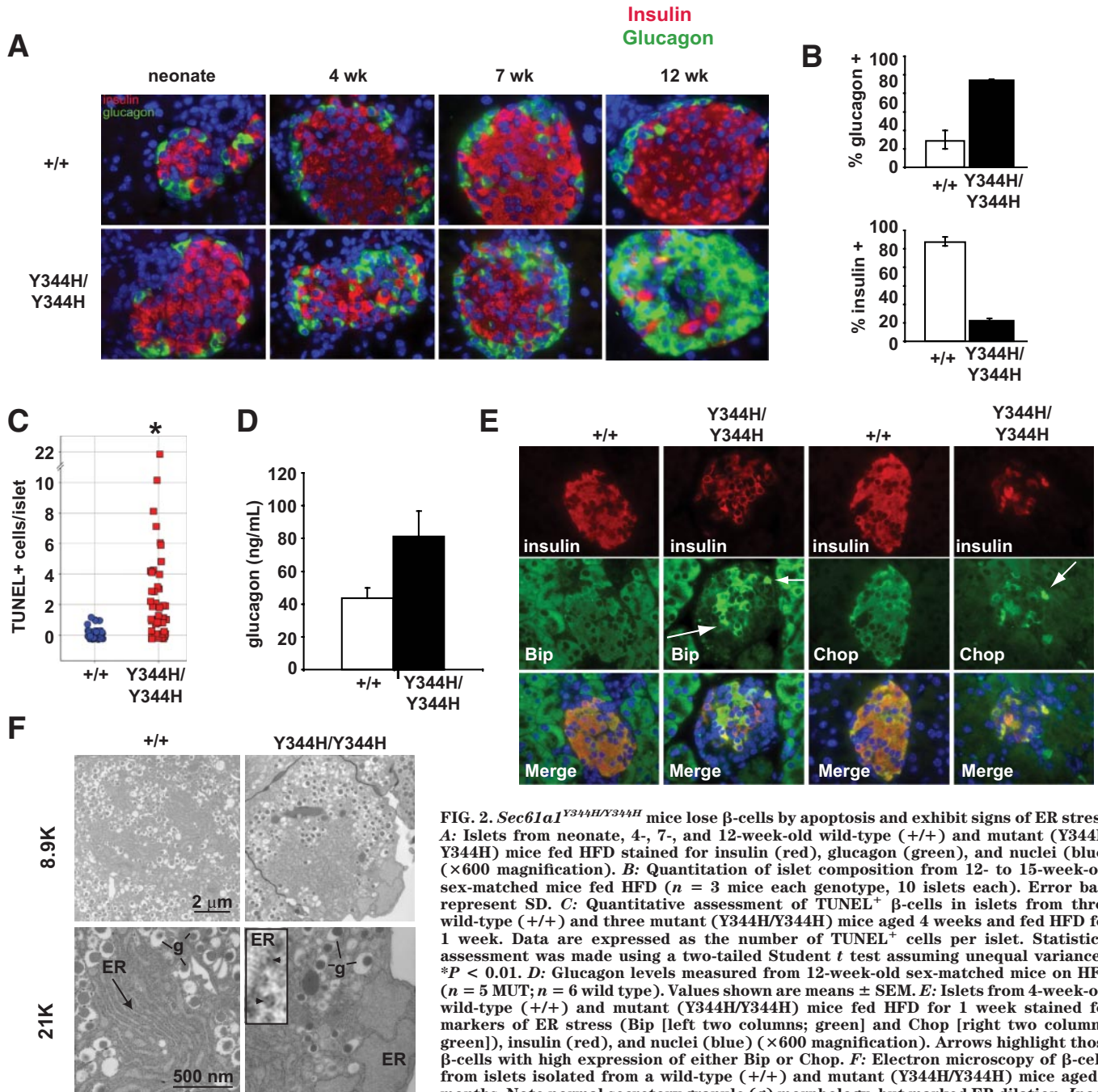


FIG. 1. *Sec61a1* is a conserved  $\beta$ -cell gene whose mutation is associated with diabetes due to hypoinulinemia. **A**: Amino acid comparison of mouse *Sec61a1* residues 330–360 to the paralog *mSec61a2* and orthologs (h, human; x, *Xenopus*; y, yeast; b, bacteria). The asterisk shows Tyr344. **B**: Fasted plasma glucose and insulin were analyzed in *Sec61a1*<sup>+/+</sup> (wild type), *Sec61a1*<sup>+/<sup>Y344H</sup></sup> (HET), and *Sec61a1*<sup>Y344H/Y344H</sup> (MUT) mice, aged 12 weeks, fed HFD. Males ( $n = 4$ –10); females ( $n = 9$ –13). Values shown are means  $\pm$  SEM. Statistical assessments were made using a two-tailed Student *t* test assuming unequal variances (versus sex-matched wild-type littermates); \* $P < 0.01$ , \*\* $P < 0.001$ . **C**: Glucose levels are elevated early in *Sec61a1*<sup>Y344H/Y344H</sup> mice (squares) compared with *Sec61a1*<sup>+/+</sup> (diamonds) animals. Values shown are means  $\pm$  SEM. Statistical assessments were made using a two-tailed Student *t* test assuming unequal variances (versus wild-type littermates). **D**: Immunohistochemistry in islets shows *Sec61a1* (middle) is highly expressed specifically in  $\beta$ -cells (as shown by insulin staining). Merged image shows colocalization. Slides were counterstained with DAPI ( $\times 200$  magnification). **E**: qPCR of *Sec61a1* from RNA isolated from islets ( $n = 4$ ) and whole pancreas ( $n = 3$ ) in age- and sex-matched *Sec61a1*<sup>+/+</sup> mice. Relative expression levels of the indicated genes were determined by comparative threshold cycle (Ct) analysis. Values shown are means  $\pm$  SD. Statistical assessment was made using a two-tailed Student *t* test assuming unequal variances. \* $P < 0.01$ . **F**: qPCR of *Sec61a1* and *Sec61a2* from age- and sex-matched *Sec61a1*<sup>+/+</sup> and *Sec61a1*<sup>Y344H/Y344H</sup> mice ( $n = 2$  each genotype). Relative expression levels were determined by comparative Ct analysis. Values shown are means  $\pm$  SD. (A high-quality color representation of this figure is available in the online issue.)



**FIG. 2.** *Sec61a1*<sup>Y344H/Y344H</sup> mice lose  $\beta$ -cells by apoptosis and exhibit signs of ER stress. **A:** Islets from neonate, 4-, 7-, and 12-week-old wild-type (+/+) and mutant (Y344H/Y344H) mice fed HFD stained for insulin (red), glucagon (green), and nuclei (blue) ( $\times 600$  magnification). **B:** Quantitation of islet composition from 12- to 15-week-old sex-matched mice fed HFD ( $n = 3$  mice each genotype, 10 islets each). Error bars represent SD. **C:** Quantitative assessment of TUNEL<sup>+</sup>  $\beta$ -cells in islets from three wild-type (+/+) and three mutant (Y344H/Y344H) mice aged 4 weeks and fed HFD for 1 week. Data are expressed as the number of TUNEL<sup>+</sup> cells per islet. Statistical assessment was made using a two-tailed Student *t* test assuming unequal variances.  $*P < 0.01$ . **D:** Glucagon levels measured from 12-week-old sex-matched mice on HFD ( $n = 5$  MUT;  $n = 6$  wild type). Values shown are means  $\pm$  SEM. **E:** Islets from 4-week-old wild-type (+/+) and mutant (Y344H/Y344H) mice fed HFD for 1 week stained for markers of ER stress (Bip [left two columns; green] and Chop [right two columns; green]), insulin (red), and nuclei (blue) ( $\times 600$  magnification). Arrows highlight those  $\beta$ -cells with high expression of either Bip or Chop. **F:** Electron microscopy of  $\beta$ -cells from islets isolated from a wild-type (+/+) and mutant (Y344H/Y344H) mice aged 6 months. Note normal secretory granule (g) morphology, but marked ER dilation. *Inset:* blowup of the ER membrane demonstrating ribosomes (arrowheads) free in the cytosol and bound to the ER membrane. (A high-quality digital representation of this figure is available in the online issue.)

hypertriglyceridemic, and exhibited hepatomegaly and steatosis, and, in older mice, hepatic cirrhosis was evident (supplementary Fig. 2).

**Loss of  $\beta$ -cells is due to apoptosis in *Sec61a1* mutant mice.** Because hyperglycemic *Sec61a1*<sup>Y344H/Y344H</sup> mice had low circulating insulin concentrations, we chose to focus on the cellular composition of the pancreatic islets of Langerhans. *Sec61a1*<sup>Y344H/Y344H</sup> mice were born with islets composed of a typical population of  $\alpha$ - and  $\beta$ -cells (Fig. 2A). However, by 3 months of age (after HFD feeding), there was a dramatic reversal of the  $\alpha$ - and  $\beta$ -cell populations in *Sec61a1*<sup>Y344H/Y344H</sup> mice. Only 15% of cells in islets from *Sec61a1*<sup>Y344H/Y344H</sup> mice were  $\beta$ -cells, in contrast to 80% in a wild-type mouse islet (Fig. 2B). We

also observed an increase in the number of somatostatin-expressing  $\delta$ -cells (supplementary Fig. 3A). These additional  $\delta$ -cells were found to be mislocalized to the interior of the islet, rather than their typical peripheral position. The  $\beta$ -cell loss, insulin insufficiency, and development of hyperglycemia are characteristic of type 1 diabetes, and immune destruction within islets. We did not, however, detect any evidence of insulinitis in islets from *Sec61a1*<sup>Y344H/Y344H</sup> mice (data not shown). We did observe multiple apoptotic  $\beta$ -cells in islets from mutant mice (Fig. 2C), but not in islets from wild-type mice. Consistent with increased apoptosis, we also detected cells positive for activated caspase-3 in *Sec61a1*<sup>Y344H/Y344H</sup> islets (supplementary Fig. 3B) but not in wild-type. This increase in

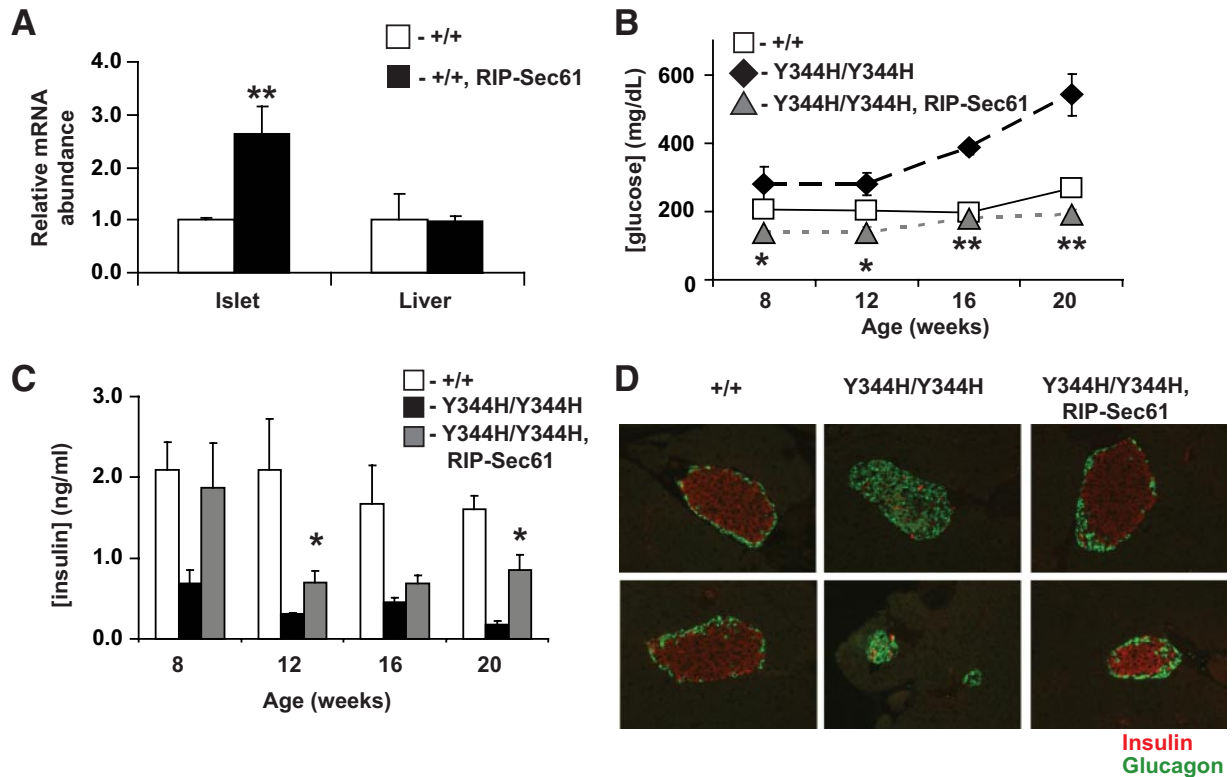


**FIG. 3.** Transgenic rescue of diabetes in mutant mice by  $\beta$ -cell-specific expression of wild-type *Sec61a1*. **A:** Expression as assessed by qPCR of *Sec61a1* in islets or liver of wild-type animals or animals transgenic for *Sec61a1* driven by the rat insulin promoter (+/+, RIP-*Sec61*);  $n = 3$  mice of each genotype, each measured in triplicate. Values shown are means  $\pm$  SEM among animals of the same genotype. Statistical assessments were made using a single-factor (genotype) ANOVA; \*\* $P < 0.001$ . **B and C:** Glucose (**B**) and insulin (**C**) in male HFD-fed *Sec61a1*<sup>+/+</sup> (+/+), *Sec61a1*<sup>Y344H/Y344H</sup> (Y344H/Y344H), and *Sec61a1*<sup>Y344H/Y344H</sup>, Tg[RIP-*Sec61*] (Y344H/Y344H, RIP-*Sec61*) mice at the indicated ages. Four males were measured for each genotype and the values shown are means  $\pm$  SEM. Statistical assessments were made using a two-tailed Student *t* test assuming unequal variances (versus mutant littermates); \* $P < 0.05$ , \*\* $P < 0.005$ . **D:** Pancreata from 24-week-old *Sec61a1*<sup>+/+</sup> (+/+), *Sec61a1*<sup>Y344H/Y344H</sup> (Y344H/Y344H), and *Sec61a1*<sup>Y344H/Y344H</sup>, Tg[RIP-*Sec61*] (Y344H/Y344H, RIP-*Sec61*) mice stained for insulin (red) and glucagon (green) ( $\times 400$  magnification). (A high-quality digital representation of this figure is available in the online issue.)

$\alpha$ -cell mass was accompanied by a trend toward higher levels of glucagon in the plasma of fasting HFD-fed mice, although this did not reach significance, which could possibly contribute to the hyperglycemic phenotype (Fig. 2D).

**ER stress in *Sec61a1* mutant mice.** Because *Sec61a1* plays a role in ER function and protein processing, we investigated ER stress in *Sec61a1*<sup>Y344H/Y344H</sup> islets. Immunohistochemical staining of islets from 4-week-old *Sec61a1*<sup>Y344H/Y344H</sup> mice showed that the ER stress markers Bip and Chop were upregulated in  $\beta$ -cells from mutant mice (Fig. 2E arrows) compared with  $\beta$ -cells from wild-type littermates. ER stress was also assessed by electron microscopy of individual *Sec61a1*<sup>Y344H/Y344H</sup>  $\beta$ -cells. Consistent with the upregulation of Bip and Chop, the ER of mutant  $\beta$ -cells was massively distended with large pools of ER lumen easily visible (Fig. 2F). Thus, the increased apoptosis in *Sec61a1*<sup>Y344H/Y344H</sup> islets was associated with increased ER stress. Note also that ribosomes engaged the ER despite a mutation in *Sec61a1* (Fig. 2F, high-magnification inset).

**Islet-specific expression of wild-type *Sec61a1* rescues diabetes and  $\beta$ -cell apoptosis but not liver pathology.** To confirm a causative role for the Y344H mutation in  $\beta$ -cell death and diabetes, we attempted to rescue the diabetic phenotype in mutant mice by expressing wild-type *Sec61a1* specifically in  $\beta$ -cells using the rat insulin promoter (RIP-*Sec*, supplementary Fig. 4) (15). Transgene-specific RT-PCR showed expression of the

transgene specifically in islets (supplementary Fig. 4C), whereas qPCR, which does not distinguish between the endogenous gene product and the product of the transgene, showed increased expression of *Sec61a1* in  $\beta$ -cells, but not liver, of transgenic animals compared with wild type (Fig. 3A). Hyperglycemia was apparent in 8-week-old HFD *Sec61a1*<sup>Y344H/Y344H</sup> mice compared with *Sec61a1*<sup>+/+</sup> controls and becomes progressively worse through 20 weeks, but mutant mice that express the RIP-*Sec* transgene (*Sec61a1*<sup>Y344H/Y344H</sup>, Tg[RIP-*Sec61*]) maintained normal glycemia throughout the 20-week time course of the experiment (Fig. 3B). Compared with wild-type controls, mutant mice were hypoinsulinemic between 8 and 20 weeks (Fig. 3C). Although insulin levels in *Sec61a1*<sup>Y344H/Y344H</sup>, Tg[RIP-*Sec61*] mice were lower than wild-type mice during this time, insulin secretion was sufficient to maintain normal glycemia up to 20 weeks of age (Fig. 3B and C). Because hyperglycemia and hypoinsulinemia in mutant mice were due to a loss of  $\beta$ -cells, we next asked whether transgenesis would rescue  $\beta$ -cell loss. At 24 weeks of age, mutant mice possessed far fewer  $\beta$ -cells compared with wild-type mice, with a concomitant expansion of glucagon-secreting  $\alpha$ -cells. This  $\beta$ -cell loss, however, was blocked by transgenic expression of wild-type *Sec61a1* (Fig. 3D).

The other prominent phenotype of mutant mice was hepatic steatosis, cirrhosis, and hepatomegaly (supplementary Fig. 2). These liver phenotypes could be a primary result of *Sec61a1* mutation in the liver or they could be

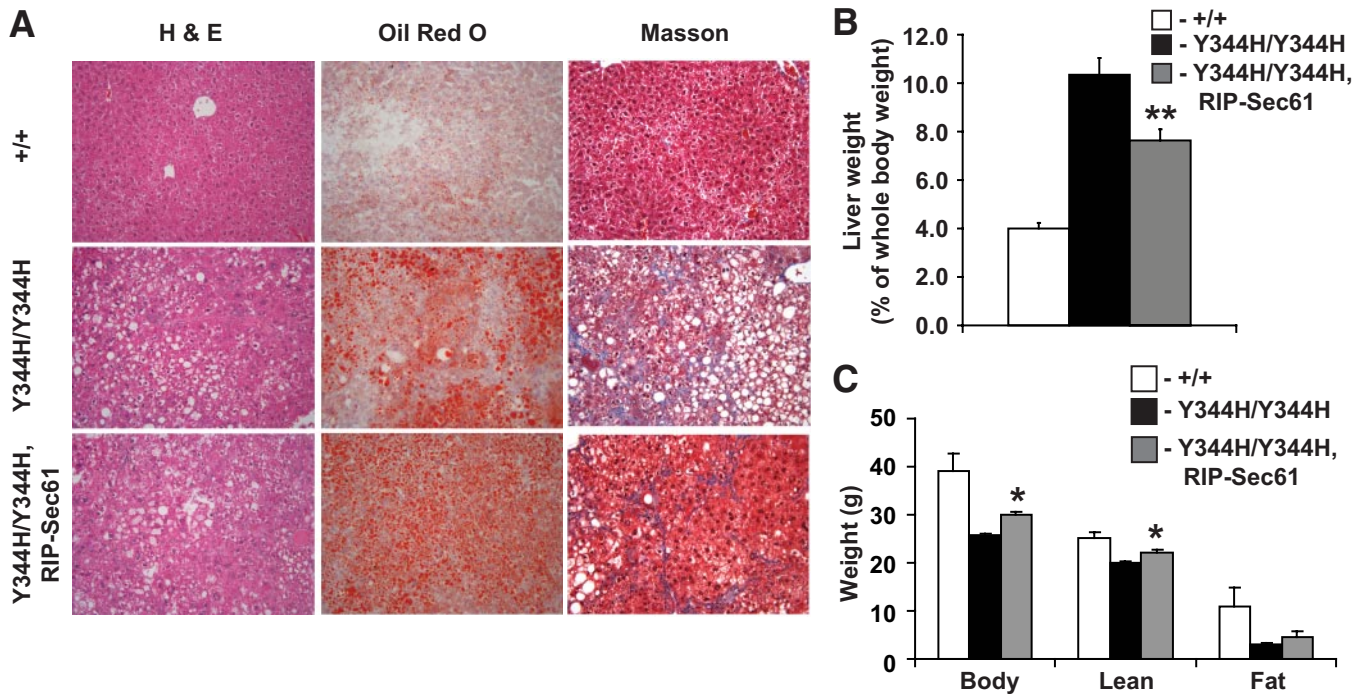


**FIG. 4.** Failure to rescue hepatic steatosis in mutant mice by  $\beta$ -cell-specific expression of wild-type *Sec61a1*. **A:** Hematoxylin-eosin (H & E, left), oil red O (middle), and Masson (right) staining of liver from *Sec61a1*<sup>+/+</sup> (+/+), *Sec61a1*<sup>Y344H/Y344H</sup> (Y344H/Y344H), and *Sec61a1*<sup>Y344H/Y344H</sup>, Tg[RIP-Sec61] (Y344H/Y344H, RIP-Sec61) mice. **B:** Hepatomegaly was assessed by dissecting and weighing liver from four males each of *Sec61a1*<sup>+/+</sup> (+/+), *Sec61a1*<sup>Y344H/Y344H</sup> (Y344H/Y344H), and *Sec61a1*<sup>Y344H/Y344H</sup>, Tg[RIP-Sec61] (Y344H/Y344H, RIP-Sec61) mice. The liver weight is expressed as a percentage of total body weight (mean  $\pm$  SEM). Statistical assessments were made using a two-tailed Student *t* test assuming unequal variances (versus wild-type littermates); \*\**P* < 0.001. **C:** Body composition in 24-week-old HFD-fed male *Sec61a1*<sup>+/+</sup> (+/+), *Sec61a1*<sup>Y344H/Y344H</sup> (Y344H/Y344H), and *Sec61a1*<sup>Y344H/Y344H</sup>, Tg[RIP-Sec61] (Y344H/Y344H, RIP-Sec61) mice. Four males were measured for each genotype and the values shown are means  $\pm$  SEM. Statistical assessments were made using a two-tailed Student *t* test assuming unequal variances (versus sex-matched mutant littermates); \**P* < 0.05. (A high-quality digital representation of this figure is available in the online issue.)

secondary to a lack of insulin signaling (16). To distinguish between these possibilities, we examined livers of *Sec61a1*<sup>+/+</sup>, *Sec61a1*<sup>Y344H/Y344H</sup>, and *Sec61a1*<sup>Y344H/Y344H</sup>, Tg[Rip-Sec61] mice. Although RIP-Sec61 transgenesis rescued diabetes, it did not affect steatosis or cirrhosis (Fig. 4A). Likewise hepatomegaly was only mildly affected by RIP-Sec61 transgenesis (Fig. 4B).

Transgenic rescue of the body weight and fat mass deficits of mutant mice was only partial, as  $\beta$ -cell-specific expression of wild-type *Sec61a1* increased the body weight and lean mass of mutants but not to the level of wild-type mice (Fig. 4C).

**RIP-Sec61 transgenesis protects  $\beta$ -cells but not hepatocytes from ER stress.** We next examined  $\beta$ -cells and hepatocytes of *Sec61a1*<sup>+/+</sup>, *Sec61a1*<sup>Y344H/Y344H</sup>, and *Sec61a1*<sup>Y344H/Y344H</sup>, Tg[Rip-Sec61] for signs of ER stress. Because HFD can itself lead to ER stress in the liver (17), we conducted these experiments on chow diet to avoid any confounding influence of HFD. Mice still develop hyperglycemia, hypoinsulinemia, glucose intolerance, and  $\beta$ -cell loss on chow diet (supplementary Table 1, supplementary Fig. 5, and data not shown). ER in mutant  $\beta$ -cells was severely distended compared with wild-type  $\beta$ -cells (Fig. 5A, center and left). This ER distension was almost completely rescued by transgenesis, with slight distension of the ER still visible by electron microscopy (Fig. 5A, right). Consistent with the rescue of ER stress shown by electron microscopy, mRNA of the ER stress response genes *Bip* and *Chop* was not elevated in islets from *Sec61a1*<sup>Y344H/Y344H</sup>, Tg[Rip-Sec61] mice compared with wild-type mice (Fig. 5B) at 3 months of age. In fact, there was a small but

significant decrease in *Chop* expression in rescued mice (Fig. 5B).

ER in mutant livers was also distended compared with wild-type liver (Fig. 5C, center) and transgenic expression of wild-type *Sec61a1* in  $\beta$ -cells did not noticeably affect this distension (Fig. 5C, right). Finally, qPCR for *Bip* and *Chop* revealed upregulation of both these genes in *Sec61a1*<sup>Y344H/Y344H</sup> and *Sec61a1*<sup>Y344H/Y344H</sup>, Tg[Rip-Sec61] mice compared with wild type (Fig. 5D). These data illustrate that sufficient expression of wild-type *Sec61a1* protects  $\beta$ -cells from ER stress present in *Sec61a1*<sup>Y344H/Y344H</sup> mice. Furthermore, these data support the notion that steatosis and hepatomegaly in this model are a direct result of *Sec61a1* mutation and ER stress in the liver, and not secondary to diabetes.

***Sec61a1*<sup>Y334H</sup> sensitizes  $\beta$ -cells to ER stress but does not affect insulin processing.** We next examined the effect that *Sec61a1*<sup>+</sup> and *Sec61a1*<sup>Y334H</sup> have on  $\beta$ -cells in vitro. For this, we cloned both *Sec61a1*<sup>+</sup> and *Sec61a1*<sup>Y334H</sup> into expression vectors and overexpressed each in a physiologically relevant  $\beta$ -cell line. MIN6 cells were ideal for this purpose as we were able to establish relatively high levels of transient transfection ( $\sim$ 50%, data not shown) and these cells maintain the ability to secrete insulin in response to high glucose concentration (18).

First, we wanted to establish whether overexpression of *Sec61a1*<sup>Y334H</sup> led to ER stress in Min6 cells. For this, we used two different luciferase-based promoter activation assays and Western blot for phosphorylated Eif2 $\alpha$ . These assays were chosen to allow us to delineate activation of different arms of the ER stress response, because in

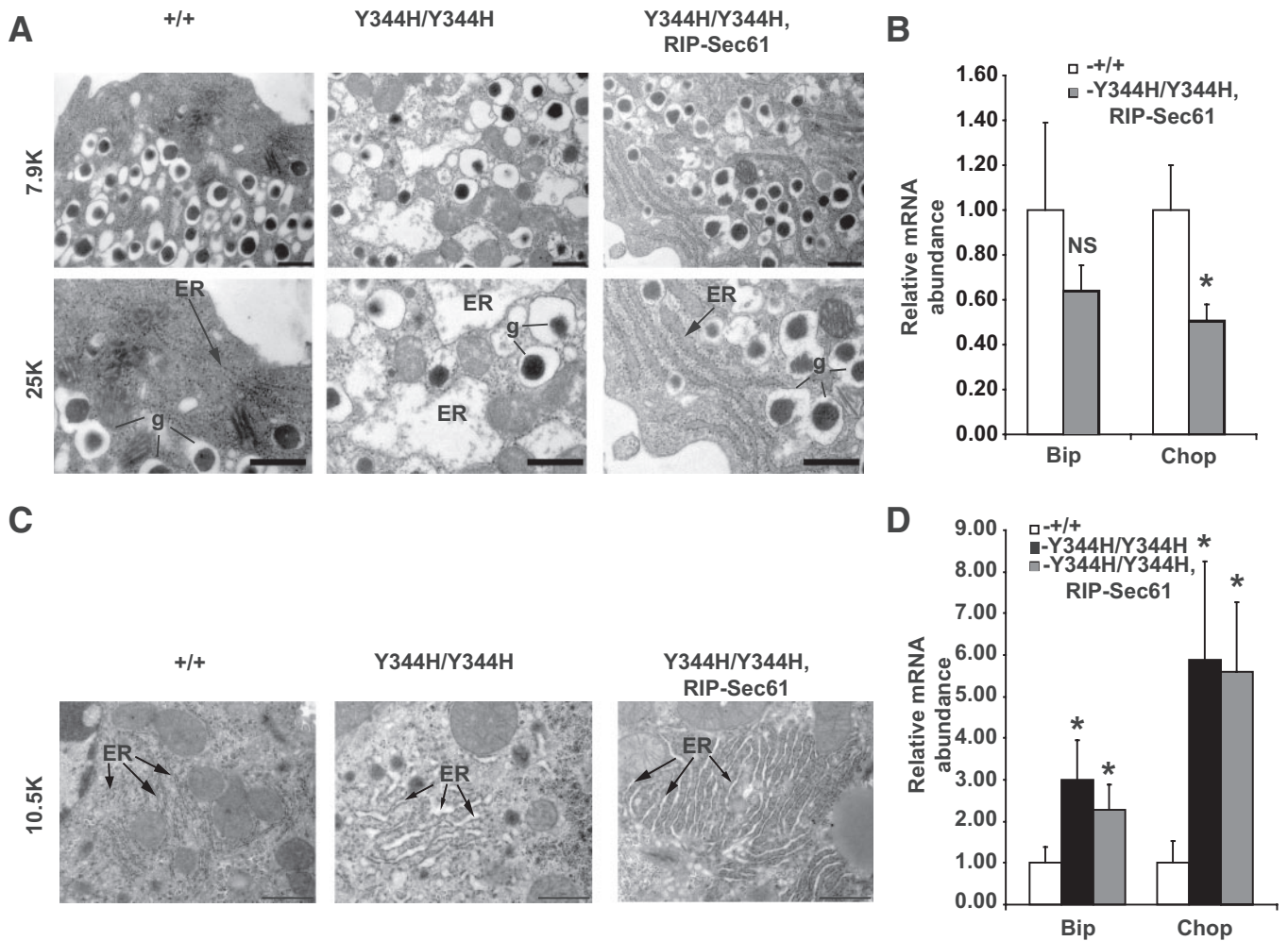


**FIG. 5.** Transgenic rescue of *Sec61 $\alpha$ 1*<sup>Y344H/Y344H</sup> normalizes signs of ER stress in  $\beta$ -cells but not hepatocytes. **A:** Electron microscopy of  $\beta$ -cells from islets isolated from *Sec61 $\alpha$ 1*<sup>+/+</sup> (+/+), *Sec61 $\alpha$ 1*<sup>Y344H/Y344H</sup> (Y344H/Y344H), and *Sec61 $\alpha$ 1*<sup>Y344H/Y344H</sup>, Tg[RIP-Sec61] (Y344H/Y344H, RIP-Sec61) mice. Bar, 1  $\mu$ m. g, secretory granules. **B:** qPCR on islets from *Sec61 $\alpha$ 1*<sup>+/+</sup> (+/+) and *Sec61 $\alpha$ 1*<sup>Y344H/Y344H</sup>, Tg[RIP-Sec61] (Y344H/Y344H, RIP-Sec61) mice. Total RNA was extracted from isolated islets of age- and sex-matched mice from each genotype ( $n = 2$ ). Relative expression levels of the indicated genes were determined by comparative Ct analysis. Values shown are means  $\pm$  SD. Statistical assessments were made using a two-tailed Student  $t$  test assuming unequal variances. \* $P < 0.01$ . **C:** Electron microscopy of livers from *Sec61 $\alpha$ 1*<sup>+/+</sup> (+/+), *Sec61 $\alpha$ 1*<sup>Y344H/Y344H</sup> (Y344H/Y344H), and *Sec61 $\alpha$ 1*<sup>Y344H/Y344H</sup>, Tg[RIP-Sec61] (Y344H/Y344H, RIP-Sec61) mice. Bar, 1  $\mu$ m. **D:** qPCR on livers from *Sec61 $\alpha$ 1*<sup>+/+</sup> (+/+), *Sec61 $\alpha$ 1*<sup>Y344H/Y344H</sup> (Y344H/Y344H), and *Sec61 $\alpha$ 1*<sup>Y344H/Y344H</sup>, Tg[RIP-Sec61] (Y344H/Y344H, RIP-Sec61) mice. Total RNA was extracted from livers of age- and sex-matched mice from each genotype ( $n = 2$ ). Relative expression levels of the indicated genes were determined by comparative Ct analysis. Values shown are means  $\pm$  SD. Statistical assessments were made using a two-tailed Student  $t$  test assuming unequal variances. \* $P < 0.01$ .

mammals the ER stress response is propagated through three different sentinels Ire-1, Atf6, and Perk (19). Eif2 $\alpha$  phosphorylation is a direct consequence of Perk activation, the ER stress response element (ERSE) is preferentially activated by Atf6 binding, and the unfolded protein response element (UPRE) is activated by Xbp-1, which is activated by Ire-1 in response to ER stress (20,21). MIN6 cells were cotransfected with plasmids expressing FLAG-tagged Sec61<sup>+</sup>, Sec61<sup>Y344H</sup>, or empty vector, and a luciferase reporter vector containing either the ERSE element or the UPRE element. We also included *Renilla* luciferase under the control of the cytomegalovirus (CMV) promoter to serve as an internal control for transfection efficiency and cell viability. Cells were then treated with thapsigargin, a pharmacological inducer of ER stress, followed by quantitation of firefly and *Renilla* luciferase activity. Interestingly, overexpression of Sec61 $\alpha$ 1<sup>Y344H</sup> significantly increased signaling through UPRE compared with Sec61 $\alpha$ 1<sup>+</sup>- or vector-transfected Min6 cells, both under basal conditions and in response to the ER stress-inducer thapsigargin (Fig. 6A). The effect of Sec61 $\alpha$ 1 on the ERSE

reporter is less clear as neither Sec61 $\alpha$ 1<sup>+</sup> nor Sec61 $\alpha$ 1<sup>Y344H</sup> overexpression increased signaling through this response element. Sec61 $\alpha$ 1<sup>+</sup>, however, reduced signaling through ERSE in response to thapsigargin-induced ER stress and Sec61 $\alpha$ 1<sup>Y344H</sup> was less effective at mitigating ER stress signaling in this pathway (Fig. 6A). To examine Perk activation via Eif2 $\alpha$  phosphorylation we transfected Min6 cells with Sec61<sup>+</sup>, Sec61<sup>Y344H</sup>, or empty vector and treated them with thapsigargin for 4 h. Western blot analysis using a phospho-specific antibody revealed enhanced Eif2 $\alpha$  phosphorylation in Min6 transfected with Sec61 $\alpha$ 1<sup>Y344H</sup> (Fig. 6B). Quantifying the Western signals showed that thapsigargin increased phosphorylation of Eif2 $\alpha$  almost 50% more in the presence of Sec61 $\alpha$ 1<sup>Y344H</sup> than in the presence of wild-type Sec61 $\alpha$ 1 (Fig. 6B).

These results indicated that mutant Sec61 $\alpha$ 1 sensitized Min6 cells to the effects of ER stress. Because Sec61 $\alpha$ 1 mediates entry into the secretory pathway and insulin is the major protein secreted from  $\beta$ -cells, we sought to determine whether aberrant insulin processing might lead

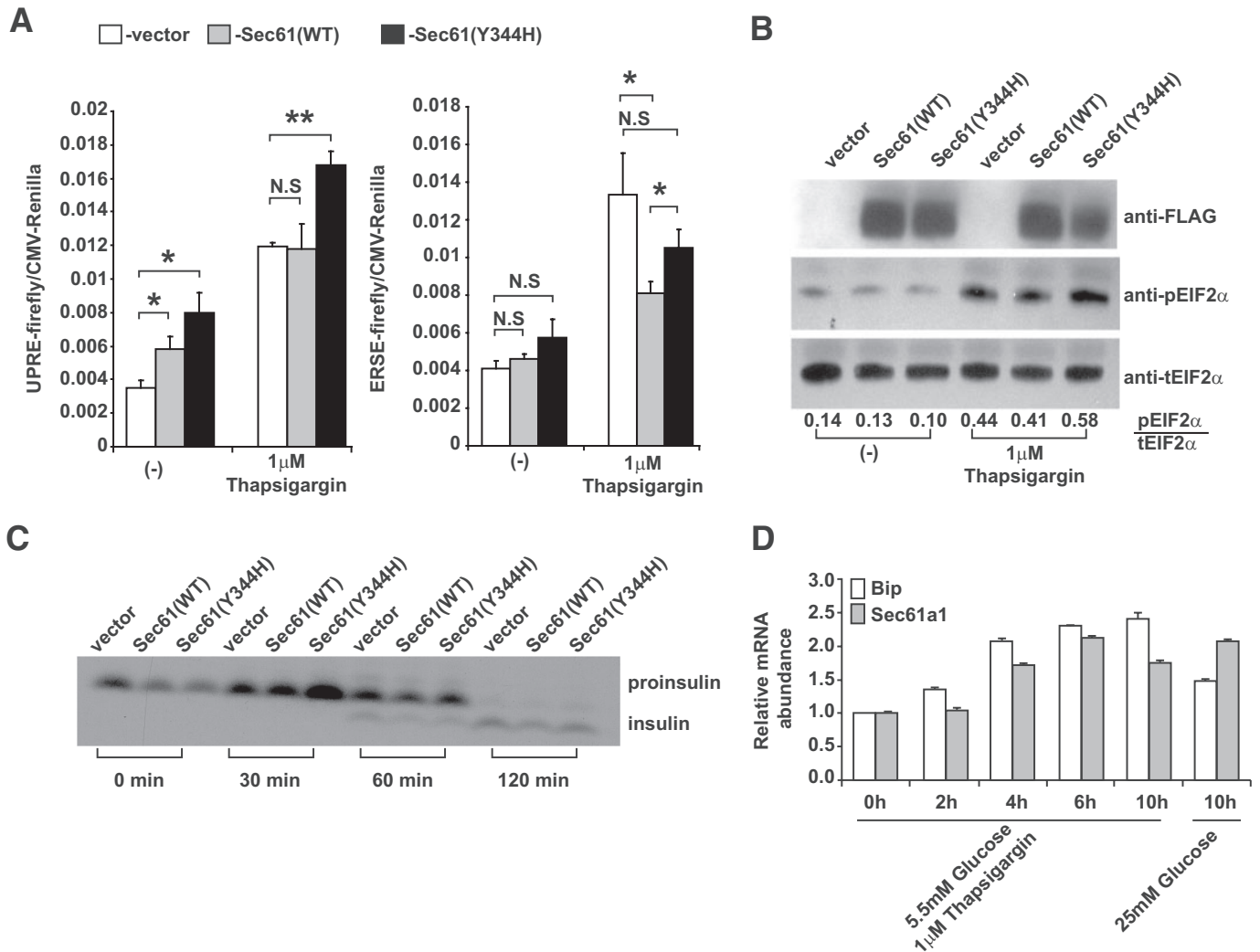


**FIG. 6.** Mutant Sec61 $\alpha$ 1 sensitizes MIN6 cells to the effects of ER stress. **A:** MIN6 cells were transfected with either ERSE (left) or UPRE (right) firefly luciferase plasmid, the indicated Sec61 expression plasmid, and a CMV *Renilla* luciferase reporter plasmid treated with 1  $\mu$ M thapsigargin and assayed for reporter activation after 16 h using a luminometer. Assays were performed in triplicate and normalized to CMV *Renilla* activity. Values represent the means  $\pm$  SD. **B:** MIN6 cells were transfected with the indicated Sec61 expression plasmid and then treated with 1  $\mu$ M thapsigargin for 4 h. Cells were lysed and Western blotting was performed with the indicated antibodies. Quantification of the Western signals is shown below the blots. **C:** Pulse-chase analysis of insulin processing in MIN6 cells transfected with the indicated expression plasmids. Cells were labeled for 20 min with 50  $\mu$ Ci of  $^{35}$ S-labeled Met and chased for the indicated time points. The upper band corresponds to proinsulin, whereas the lower band corresponds to the fully processed form. **D:** *Sec61a1* and *Bip* gene expression in the MIN6  $\beta$ -cell line and their upregulation in cells cultured in high-glucose media or in the presence of the ER stress-inducer thapsigargin (Tg). The x-axis shows the time in hours after the initial exposure of the cells to Tg or high glucose. Relative expression levels were determined by comparative Ct analysis. Values represent means  $\pm$  SD.

to ER stress in Min6 cells. We transfected cells with vector, Sec61<sup>+</sup>, or Sec61<sup>Y344H</sup>, labeled them with  $^{35}$ S-labeled Cys, and assayed insulin processing 0, 30, 60, and 120 min after chase with unlabeled Cys to determine whether insulin processing was influenced by the mutant Sec61. Because insulin is translated as a single polypeptide (proinsulin) and not fully processed to its mature form until it is transported to secretory granules, any temporal delay in insulin processing from its pro form would indicate that insulin folding/quality control is corrupted by the mutant Sec61 protein. In fact, pulse-chase labeling of insulin revealed that there is no noticeable defect in insulin processing in cells transfected with mutant Sec61 compared with both wild-type and vector-transfected cells (Fig. 6C). These results indicate that ER stress apparent in both primary  $\beta$ -cells and  $\beta$ -cell lines as a result of mutant Sec61 is not a result of improper folding, quality control, or transport of insulin.

Finally, given the effect Sec61 $\alpha$ 1 had on ER stress signaling in MIN6 cells we next wanted to know whether Sec61 $\alpha$ 1 is regulated in response to ER stress or high glucose. MIN6 cells were cultured in low-glucose DMEM and treated with thapsigargin. A time course of mRNA levels for *Sec61a1* indicates that this gene is upregulated in response to ER stress concomitant with *Bip*, a canonical ER stress response gene (Fig. 6D). Furthermore, the level of *Sec61a1* and *Bip* mRNA reached after 10 h of thapsigargin treatment is equivalent to that of 10 h of culture in high-glucose DMEM (Fig. 6D, right).

## DISCUSSION

In this report we have used ENU mutagenesis to identify a mutation in the *Sec61a1* gene that leads to diabetes and hepatosteatosis in homozygous mutant mice. Diabetes in this model is a result of insulin insufficiency that is caused

by a loss of  $\beta$ -cells due to apoptosis. We found that apoptosis was a result of ER stress in pancreatic islets, and that islet-specific expression of wild-type Sec61 $\alpha$ 1 not only rescued hyperglycemia and the  $\beta$ -cell composition of islets in mutant mice, but also rescued ER stress. Experiments in vitro in MIN6 cells reveal that Sec61<sup>Y3344H</sup> is directly responsible for a dysregulated ER stress response in  $\beta$ -cells. Furthermore, we have shown that *Sec61a1* is an ER stress response gene in  $\beta$ -cells, and is responsive to high glucose conditions.

Sec61 $\alpha$ 1 mutation also led to ER stress in hepatocytes as evidenced by electron microscopy and qPCR. TUNEL staining revealed that elevated ER stress led to a higher rate of apoptosis in hepatocytes from mutant mice (supplementary Fig. 6A), however, in this case, apoptosis was compensated for by increased proliferation in mutant mice (supplementary Fig. 6B) as indicated by bromodeoxyuridine incorporation. Thus, through islet-specific rescue of diabetes we have also uncovered a fatty liver phenotype that is a primary result of Sec61 $\alpha$ 1 mutation and ER stress, not hyperglycemia.

Because Sec61 $\alpha$ 1 is involved in the translocation of newly synthesized polypeptides into the ER lumen, it is likely that some protein important for  $\beta$ -cell function is being improperly folded, partitioned into the membrane, or transported from the ER. A likely culprit in  $\beta$ -cells is misfolded/misprocessed insulin. The presence of dense staining secretory granules, however, being normal in both number and appearance, in electron micrographs (Fig. 2F) suggests that formation of insulin secretory granules is unaffected in mutants, and pulse labeling in MIN6 cells (Fig. 6C) indicates insulin processing is unaffected by this particular Sec61 $\alpha$ 1 point mutant. Additionally, the insulin in these  $\beta$ -cells is fully processed and disulfide bonded as determined by nonreducing PAGE of islet lysates from 4-week-old *Sec61a1*<sup>Y344H/Y344H</sup> mice prior to complete  $\beta$ -cell loss (supplementary Fig. 7). This is in contrast to a situation in which defects in the production and secretion of mature insulin leads to glucose intolerance due to a defective response to ER stress (22). In this case a serine in Eif2 $\alpha$  is substituted with alanine (S51A) such that Eif2 $\alpha$  is not phosphorylated by Perk, and translation is not attenuated, in response to ER stress. This failure to attenuate translation in the face of increased secretory burden of the  $\beta$ -cell brought on by diet-induced insulin resistance leads to a saturation of the ER's capacity to fold and process proteins, in turn leading to a reduction of insulin in secretory granules (22). Likewise, the observation that mice respond to intraperitoneal injection of insulin implies that insulin receptor and GLUT trafficking is not impaired in mutant mice (supplementary Fig. 5A).

Rather than a defect in ER import or secretion of insulin or some component necessary for  $\beta$ -cell survival, our data suggest that  $\beta$ -cell apoptosis is due to generalized ER stress. ER stress is caused by the accumulation of unfolded proteins in the ER (19). The cell responds to ER stress by 1) attenuating translation, 2) increasing the capacity of the ER to process proteins, by upregulating folding chaperones, and 3) increasing the rate at which unfolded proteins are removed and degraded. Collectively, these adaptations are called the unfolded protein response (UPR) (19). If the UPR does not relieve ER stress, apoptosis occurs, and in the case of  $\beta$ -cell loss, diabetes develops.

An increasing body of evidence has shown that the  $\beta$ -cell is sensitive to ER stress (23–25). Indeed ER stress has been implicated in several monogenic forms of diabe-

tes in humans. These include two human pleiotropic syndromes associated with early-onset diabetes, Wolfram syndrome (caused by mutations in *WFS1*) (26,27) and Wolcott-Rallison syndrome (caused by mutations in *EIF2AK3/PERK*) (28,29), and neonatal diabetes caused by mutations in the proinsulin gene itself (30–32), which prevent proper folding and/or disulfide bonding of mature insulin. Recently, several studies have shown an association between the development of type 2 diabetes and variation in the *WFS1* gene (33,34). ER stress and  $\beta$ -cell apoptosis have also been linked to diabetes in human autopsy studies showing an increase in CHOP staining and ER expansion (35,36). Furthermore islets from diabetic individuals show elevation of ER stress markers *BIP*, *CHOP*, and *XBPI* in response to high glucose conditions to a greater extent than in nondiabetic subjects (37).

This particular mutation in Sec61 $\alpha$ 1 occurs in a dityrosine motif that is conserved in the Sec61 $\alpha$ 1 protein sequence of every homolog we have examined (sampled in Fig. 1A), suggesting that it is critical for proper function. Being positioned on the luminal side of the ER membrane, it is likely that this dityrosine facilitates an interaction with a protein involved in maintaining ER homeostasis, such as a chaperone or other protein involved in ER quality control, or that it may contribute to some catalytic function of Sec61 $\alpha$ 1 itself.

Experiments shown here indicate that Sec61 $\alpha$ 1 is upregulated in response to both ER stress and high glucose levels, indicating that Sec61 $\alpha$ 1 is part of a coordinated  $\beta$ -cell response to augmented secretory demand initiated by elevated glucose levels. In fact, recent evidence suggests that chronically elevated glucose levels lead to ER stress and an ultimate attenuation of insulin production (38,39). Glucose also leads to enhanced overall translation in  $\beta$ -cells through dephosphorylation of Eif2 $\alpha$ , apparently independent of signaling through the UPR (40) and this effect is not altered by Sec61 $\alpha$ 1<sup>Y344H</sup> in MIN6 cells (data not shown). Compromising Sec61 function only slightly could lead to a positive feedback loop in which higher levels of ER stress in response to transient hyperglycemia result in lower levels of insulin production, which leads to more severe hyperglycemia, which leads to greater stress on  $\beta$ -cells and ultimately  $\beta$ -cell failure and overt diabetes. That Sec61 $\alpha$ 1 expression is important for  $\beta$ -cell survival is supported by the observation that *Sec61a1*<sup>Y344H/Y344H</sup>, Tg [Rip-Sec61] mice exhibit significantly lower levels of *Chop* mRNA compared with wild-type mice. This is important considering genetic deletion of *Chop*, a proapoptotic transcription factor upregulated by ER stress, leads to amelioration of several models of ER stress-induced diabetes and  $\beta$ -cell loss (41).

*Sec61a1*<sup>Y344H/Y344H</sup> mice also develop hepatomegaly, hepatic steatosis, and cirrhosis, which could be secondary to a lack of insulin signaling (16) or a direct result of *Sec61a1* mutation in hepatocytes. Our data show that they are a direct result of mutation in the liver. Although it remains to be determined whether steatosis is mediated by ER stress in this model, hepatic steatosis associated with ER stress has been noted in hyperhomocysteinemic (42), genetically obese (43), HFD-fed (44,45), and genetically altered mice lacking UPR response genes (46).

In summary, we have presented genetic, physiological, and molecular evidence that Sec61 $\alpha$ 1 is important for  $\beta$ -cell survival in response to hyperglycemia, and that mutation of Sec61 $\alpha$ 1 leads to diabetes via  $\beta$ -cell apoptosis

as a result of ER stress and hepatosteatosis via ER stress. This is also, to our knowledge, the first Sec61 $\alpha$ 1 functional mutation in a mammalian system that is not lethal. In the future, this mouse model can be used to shed light on the effect of abrogated Sec61 $\alpha$ 1 function in different tissues and disease states.

#### ACKNOWLEDGMENTS

These studies were supported by a grant from the National Institutes of Health (DK-079925) to N.G.

No potential conflicts of interest relevant to this article were reported.

The authors acknowledge the contributions of Sandy Bohan for technical assistance with experiments; Lacey Kischassey for maintaining and caring for the mice used; Tim Wiltshire and Brian Steffy for mapping, sequencing, and genotyping; Malcolm Wood for the electron micrographs; Bill Kiosses for imaging bromodeoxyuridine and TUNEL staining in the liver; and Jeff Pitman and Mingyue Zhou for a critical reading of the article.

#### REFERENCES

- Kahn SE, Hull RL, Utzschneider KM. Mechanisms linking obesity to insulin resistance and type 2 diabetes. *Nature* 2006;444:840–846
- Permutt MA, Wasson J, Cox N. Genetic epidemiology of diabetes. *J Clin Invest* 2005;115:1431–1439
- Horikawa Y, Oda N, Cox NJ, Li X, Orho-Melander M, Hara M, Hinokio Y, Lindner TH, Mashima H, Schwarz PE, del Bosque-Plata L, Horikawa Y, Oda Y, Yoshiuchi I, Colilla S, Polonsky KS, Wei S, Concannon P, Iwasaki N, Schulze J, Baier LJ, Bogardus C, Groop L, Boerwinkle E, Hani S, Bell GI. Genetic variation in the gene encoding calpain-10 is associated with type 2 diabetes mellitus. *Nat Genet* 2000;26:163–175
- Sladek R, Rocheleau G, Rung J, Dina C, Shen L, Serre D, Boutin P, Vincent D, Belisle A, Hadjadj S, Balkau B, Heude B, Charpentier G, Hudson TJ, Montpetit A, Pshzhetsky AV, Prentki M, Posner BI, Balding DJ, Meyre D, Polychronakos C, Froguel P. A genome-wide association study identifies novel risk loci for type 2 diabetes. *Nature* 2007;445:881–885
- Diabetes Genetics Initiative of Broad Institute of Harvard and MIT, Lund University, and Novartis Institutes of BioMedical Research, Saxena R, Voight BF, Lyssenko V, Burtt NP, de Bakker PI, Chen H, Roix JJ, Kathiresan S, Hirschhorn JN, Daly MJ, Hughes TE, Groop L, Althuler D, Almgren P, Florez JC, Meyer J, Ardlie K, Bengtsson Boström K, Isomaa B, Lettre G, Lindblad U, Lyon HN, Melander O, Newton-Cheh C, Nilsson P, Orho-Melander M, Råstam L, Seliotes EK, Taskiran MR, Tuomi T, Guiducci C, Berglund A, Carlson J, Gianniny L, Hackett R, Hall L, Holmkvist J, Laurila E, Sjögren M, Sterner M, Surti A, Svensson M, Svensson M, Tewhey R, Blumenstiel B, Parkin M, Defelice M, Barry R, Brodeur W, Camarata J, Chia N, Fava M, Gibbons J, Handsaker B, Healy C, Nguyen K, Gates C, Sougnez C, Gage D, Nizzari M, Gabriel SB, Chirn GW, Ma Q, Parikh H, Richardson D, Rieke D, Purcell S. Genome-wide association analysis identifies loci for type 2 diabetes and triglyceride levels. *Science* 2007;316:1331–1336
- King DP, Vitaterna MH, Chang AM, Dove WF, Pinto LH, Turek FW, Takahashi JS. The mouse clock mutation behaves as an antimorph and maps within the W19H deletion, distal of Kit. *Genetics* 1997;146:1049–1060
- Keays DA, Tian G, Poirier K, Huang GJ, Siebold C, Cleak J, Oliver PL, Fray M, Harvey RJ, Molnár Z, Piñon MC, Dear N, Valdar W, Brown SD, Davies KE, Rawlins JN, Cowan NJ, Nolan P, Chelly J, Flint J. Mutations in alpha-tubulin cause abnormal neuronal migration in mice and lissencephaly in humans. *Cell* 2007;128:45–57
- Yu P, Constien R, Dear N, Katan M, Hanke P, Bunney TD, Kunder S, Quintanilla-Martinez L, Huffstadt U, Schröder A, Jones NP, Peters T, Fuchs H, de Angelis MH, Nehls M, Grosse J, Wabnitz P, Meyer TP, Yasuda K, Schiemann M, Schneider-Fresenius C, Jagla W, Russ A, Popp A, Josephs M, Marquardt A, Laufs J, Schmittwolf C, Wagner H, Pfeffer K, Mudde GC. Autoimmunity and inflammation due to a gain-of-function mutation in phospholipase C gamma 2 that specifically increases external Ca<sup>2+</sup> entry. *Immunity* 2005;22:451–465
- Graw J, Jung M, Löster J, Klopp N, Soewarto D, Fella C, Fuchs H, Reis A, Wolf E, Balling R, Hrab de Angelis M. Mutation in the betaA3/A1-crystallin encoding gene Cryba1 causes a dominant cataract in the mouse. *Genomics* 1999;62:67–73
- Toye AA, Moir L, Huggill A, Bentley L, Quarterman J, Mijat V, Hough T, Goldsworthy M, Haynes A, Hunter AJ, Browne M, Spurr N, Cox RD. A new mouse model of type 2 diabetes, produced by N-ethyl-nitrosourea mutagenesis, is the result of a missense mutation in the glucokinase gene. *Diabetes* 2004;53:1577–1583
- Wen BG, Pletcher MT, Warashina M, Choe SH, Ziaee N, Wiltshire T, Sauer K, Cooke MP. Inositol (1,4,5) trisphosphate 3 kinase B controls positive selection of T cells and modulates Erk activity. *Proc Natl Acad Sci U S A* 2004;101:5604–5609
- Wiltshire T, Pletcher MT, Batalov S, Barnes SW, Tarantino LM, Cooke MP, Wu H, Smylie K, Santrosyan A, Copeland NG, Jenkins NA, Kalush F, Mural RJ, Glynn RJ, Kay SA, Adams MD, Fletcher CF. Genome-wide single-nucleotide polymorphism analysis defines haplotype patterns in mouse. *Proc Natl Acad Sci U S A* 2003;100:3380–3385
- Lloyd DJ, Bohan S, Gekakis N. Obesity, hyperphagia and increased metabolic efficiency in Pcl mutant mice. *Hum Mol Genet* 2006;15:1884–1893
- Gilula NB, Epstein ML, Beers WH. Cell-to-cell communication and ovulation: a study of the cumulus-oocyte complex. *J Cell Biol* 1978;78:58–75
- Miyazaki J, Araki K, Yamato E, Ikegami H, Asano T, Shibasaki Y, Oka Y, Yamamura K. Establishment of a pancreatic beta cell line that retains glucose-inducible insulin secretion: special reference to expression of glucose transporter isoforms. *Endocrinology* 1990;127:126–132
- Hanahan D. Heritable formation of pancreatic beta-cell tumours in transgenic mice expressing recombinant insulin/simian virus 40 oncogenes. *Nature* 1985;315:115–122
- Michael MD, Kulkarni RN, Postic C, Previs SF, Shulman GI, Magnuson MA, Kahn CR. Loss of insulin signaling in hepatocytes leads to severe insulin resistance and progressive hepatic dysfunction. *Mol Cell* 2000;6:87–97
- Ozcan U, Cao Q, Yilmaz E, Lee AH, Iwakoshi NN, Ozdelen E, Tuncman G, Görgün C, Glimcher LH, Hotamisligil GS. Endoplasmic reticulum stress links obesity, insulin action, and type 2 diabetes. *Science* 2004;306:457–461
- Ishihara H, Asano T, Tsukuda K, Katagiri H, Inukai K, Anai M, Kikuchi M, Yazaki Y, Miyazaki JI, Oka Y. Pancreatic beta cell line MIN6 exhibits characteristics of glucose metabolism and glucose-stimulated insulin secretion similar to those of normal islets. *Diabetologia* 1993;36:1139–1145
- Schröder M, Kaufman RJ. The mammalian unfolded protein response. *Annu Rev Biochem* 2005;74:739–789
- Harding HP, Zhang Y, Ron D. Protein translation and folding are coupled by an endoplasmic-reticulum-resident kinase. *Nature* 1999;397:271–274
- Yamamoto K, Yoshida H, Kokame K, Kaufman RJ, Mori K. Differential contributions of ATF6 and XBP1 to the activation of endoplasmic reticulum stress-responsive cis-acting elements ERSE, UPRE and ERSE-II. *J Biochem (Tokyo)* 2004;136:343–350
- Scheuner D, Vander Mierde D, Song B, Flamez D, Creemers JW, Tsukamoto K, Ribick M, Schuit FC, Kaufman RJ. Control of mRNA translation preserves endoplasmic reticulum function in beta cells and maintains glucose homeostasis. *Nat Med* 2005;11:757–764
- Araki E, Oyadomari S, Mori M. Endoplasmic reticulum stress and diabetes mellitus. *Intern Med* 2003;42:7–14
- Harding HP, Ron D. Endoplasmic reticulum stress and the development of diabetes: a review. *Diabetes* 2002;51(Suppl. 3):S455–S461
- Oyadomari S, Araki E, Mori M. Endoplasmic reticulum stress-mediated apoptosis in pancreatic beta-cells. *Apoptosis* 2002;7:335–345
- Inoue H, Tanizawa Y, Wasson J, Behn P, Kalidas K, Bernal-Mizrachi E, Mueckler M, Marshall H, Donis-Keller H, Crock P, Rogers D, Mikuni M, Kumashiro H, Higashi K, Sobue G, Oka Y, Permutt MA. A gene encoding a transmembrane protein is mutated in patients with diabetes mellitus and optic atrophy (Wolfram syndrome). *Nat Genet* 1998;20:143–148
- Riggs AC, Bernal-Mizrachi E, Ohsugi M, Wasson J, Fatrai S, Welling C, Murray J, Schmidt RE, Herrera PL, Permutt MA. Mice conditionally lacking the Wolfram gene in pancreatic islet beta cells exhibit diabetes as a result of enhanced endoplasmic reticulum stress and apoptosis. *Diabetologia* 2005;48:2313–2321
- Delépine M, Nicolino M, Barrett T, Golamaully M, Lathrop GM, Julier C. EIF2AK3, encoding translation initiation factor 2-alpha kinase 3, is mutated in patients with Wolcott-Rallison syndrome. *Nat Genet* 2000;25:406–409
- Harding HP, Zeng H, Zhang Y, Jungries R, Chung P, Plesken H, Sabatini DD, Ron D. Diabetes mellitus and exocrine pancreatic dysfunction in perk-/- mice reveals a role for translational control in secretory cell survival. *Mol Cell* 2001;7:1153–1163
- Edghill EL, Flanagan SE, Patch AM, Bousted C, Parrish A, Shields B, Shepherd MH, Hussain K, Kapoor RR, Malecki M, MacDonald MJ, Støyr J, Steiner DF, Philipson LH, Bell GI, The Neonatal Diabetes International Collaborative Group, Hattersley AT, Ellard S. Insulin mutation screening in

- 1,044 patients with diabetes: mutations in the INS gene are a common cause of neonatal diabetes but a rare cause of diabetes diagnosed in childhood or adulthood. *Diabetes* 2008;57:1034–1042
31. Molven A, Ringdal M, Nordbø AM, Raeder H, Støy J, Lipkind GM, Steiner DF, Philipson LH, Bergmann I, Aarskog D, Undlien DE, Joner G, Søvik O, the Norwegian Childhood Diabetes Study Group, Bell GI, Njølstad PR. Mutations in the insulin gene can cause MODY and autoantibody-negative type 1 diabetes. *Diabetes* 2008;57:1131–1135
  32. Støy J, Edghill EL, Flanagan SE, Ye H, Paz VP, Pluzhnikov A, Below JE, Hayes MG, Cox NJ, Lipkind GM, Lipton RB, Greeley SA, Patch AM, Ellard S, Steiner DF, Hattersley AT, Philipson LH, Bell GI, the Neonatal Diabetes International Collaborative Group. Insulin gene mutations as a cause of permanent neonatal diabetes. *Proc Natl Acad Sci U S A* 2007;104:15040–15044
  33. Franks PW, Rolandsson O, Debenham SL, Fawcett KA, Payne F, Dina C, Froguel P, Mohlke KL, Willer C, Olsson T, Wareham NJ, Hallmans G, Barroso I, Sandhu MS. Replication of the association between variants in WFS1 and risk of type 2 diabetes in European populations. *Diabetologia* 2008;51:458–463
  34. Sandhu MS, Weedon MN, Fawcett KA, Wasson J, Debenham SL, Daly A, Lango H, Frayling TM, Neumann RJ, Sherva R, Blech I, Pharoah PD, Palmer CN, Kimber C, Tavendale R, Morris AD, McCarthy MI, Walker M, Hitman G, Glaser B, Permutt MA, Hattersley AT, Wareham NJ, Barroso I. Common variants in WFS1 confer risk of type 2 diabetes. *Nat Genet* 2007;39:951–953
  35. Butler AE, Janson J, Bonner-Weir S, Ritzel R, Rizza RA, Butler PC. Beta-cell deficit and increased beta-cell apoptosis in humans with type 2 diabetes. *Diabetes* 2003;52:102–110
  36. Huang C-J, Lin C-Y, Haataja L, Gurlo T, Butler AE, Rizza RA, Butler PC. High expression rates of human islet amyloid polypeptide induce endoplasmic reticulum stress-mediated beta-cell apoptosis, a characteristic of humans with type 2 but not type 1 diabetes. *Diabetes* 2007;56:2016–2027
  37. Marchetti P, Bugliani M, Lupi R, Marselli L, Masini M, Boggi U, Filipponi F, Weir GC, Eizirik DL, Cnop M. The endoplasmic reticulum in pancreatic beta cells of type 2 diabetes patients. *Diabetologia* 2007;50:2486–2494
  38. Lipson KL, Fonseca SG, Ishigaki S, Nguyen LX, Foss E, Bortell R, Rossini AA, Urano F. Regulation of insulin biosynthesis in pancreatic beta cells by an endoplasmic reticulum-resident protein kinase IRE1. *Cell Metab* 2006;4:245–254
  39. Lipson KL, Ghosh R, Urano F. The role of IRE1alpha in the degradation of insulin mRNA in pancreatic beta-cells. *PLoS ONE* 2008;3:e1648
  40. Vander Mierde D, Scheuner D, Quintens R, Patel R, Song B, Tsukamoto K, Beullens M, Kaufman RJ, Bollen M, Schuit FC. Glucose activates a protein phosphatase-1-mediated signaling pathway to enhance overall translation in pancreatic beta-cells. *Endocrinology* 2007;148:609–617
  41. Song B, Scheuner D, Ron D, Pennathur S, Kaufman RJ. Chop deletion reduces oxidative stress, improves beta cell function, and promotes cell survival in multiple mouse models of diabetes. *J Clin Invest* 2008;118:3378–3389
  42. Werstuck GH, Lentz SR, Dayal S, Hossain GS, Sood SK, Shi YY, Zhou J, Maeda N, Krisans SK, Malinow MR, Austin RC. Homocysteine-induced endoplasmic reticulum stress causes dysregulation of the cholesterol and triglyceride biosynthetic pathways. *J Clin Invest* 2001;107:1263–1273
  43. Ozcan U, Yilmaz E, Ozcan L, Furuhashi M, Vaillancourt E, Smith RO, Görgün CZ, Hotamisligil GS. Chemical chaperones reduce ER stress and restore glucose homeostasis in a mouse model of type 2 diabetes. *Science* 2006;313:1137–1140
  44. Oyadomari S, Harding HP, Zhang Y, Oyadomari M, Ron D. Dephosphorylation of translation initiation factor 2alpha enhances glucose tolerance and attenuates hepatosteatosis in mice. *Cell Metab* 2008;7:520–532
  45. Yoshiuchi K, Kaneto H, Matsuoka TA, Kohno K, Iwawaki T, Nakatani Y, Yamasaki Y, Hori M, Matsuhisa M. Direct monitoring of in vivo ER stress during the development of insulin resistance with ER stress-activated indicator transgenic mice. *Biochem Biophys Res Commun* 2008;366:545–550
  46. Rutkowski DT, Wu J, Back SH, Callaghan MU, Ferris SP, Iqbal J, Clark R, Miao H, Hassler JR, Fornek J, Katze MG, Hussain MM, Song B, Swathirajan J, Wang J, Yau GD, Kaufman RJ. UPR pathways combine to prevent hepatic steatosis caused by ER stress-mediated suppression of transcriptional master regulators. *Dev Cell* 2008;15:829–840